

# Studies on Synthesis and Characterization of Advanced Electrode Material Nanocomposite of Tetra Metal Oxides of Fe-Mn-Ni-Co-ZIF-8@rGO

<sup>\*1</sup>A. Niresha Gnana Mary, <sup>2</sup>Dr. A. S. Stella Shalini and <sup>3</sup>Dr. G. Sivasankari

<sup>1</sup>PhD Scholar, PG & Research Department of Chemistry, St. Joseph's College (Affiliated to Bharathidasan University), Tiruchirappalli-2, Tamil Nadu, India

<sup>2</sup>Associate Professor, PG & Research Department of Chemistry, St. Joseph's College (Affiliated to Bharathidasan University), Tiruchirappalli-2, Tamil Nadu, India

<sup>3</sup>Assistant Professor, PG & Research Department of Chemistry, Cauvery College, (Affiliated to Bharathidasan University), Tiruchirappalli-18, Tamil Nadu, India

\*Corresponding Author

DOI: <https://doi.org/10.51584/IJRIAS.2026.11060161>

Received: 15 June 2026; Accepted: 20 June 2026; Published: 04 July 2026

## ABSTRACT

The growing demand for efficient and sustainable energy storage systems has accelerated the development of advanced electrode materials for high-performance supercapacitors. In this study, novel nanocomposite electrodes based on zeolitic imidazolate framework-8, Fe-Mn-Ni-Co tetra-metal oxides and reduced graphene oxide were designed, synthesized and characterized to enhance electrochemical energy storage performance. The synthesized materials were systematically characterized using Fourier Transform Infrared Spectroscopy and X-ray Diffraction techniques. FTIR analysis confirmed the coexistence of characteristic organic functional groups of ZIF-8 and metal-oxygen vibrations of transition metal oxides, indicating successful hybrid composite formation. XRD studies revealed the crystalline nature and phase purity of ZIF-8 along with the formation of nanocrystalline Fe-Mn-Ni-Co oxide structures. The presence of multiple transition metal ions generated lattice distortions and increased the density of electroactive sites, thereby facilitating enhanced redox reactions. Overall, the study demonstrates that ZIF-8-derived Fe-Mn-Ni-Co oxide/rGO nanocomposites are promising electrode materials for next-generation supercapacitors.

**Keywords:** Tetra-metal oxides, Fe-Mn-Ni-Co oxide, Reduced graphene oxide (rGO), Nanocomposites, Energy storage, Electrochemical performance.

## INTRODUCTION

Electrochemical capacitors are considered more promising energy stockpiling frameworks than batteries because of their high power density (>10 kW kg<sup>-1</sup>), high rate ability, and long cycle life (>1,000,000 cycles) [1]. Electrochemical double-layer capacitors (EDLCs) and pseudocapacitors are the most common types of supercapacitors based on their energy. The energy storage mechanism in pseudocapacitors depends on redox reactions, while EDLCs rely on charge absorption on the electrode surface [2-4]. Although EDLCs exhibit good cycle stability and high conductivity, they have lower specific capacitance [5]. However, the pseudocapacitor has a superior theoretical specific capacitance and higher energy density, but its poor life cycle is a significant drawback for practical application [6]. Thus, to overcome these issues and meet the criteria for practical applications, developing novel electrode materials is crucial. There is a growing interest in advanced nanostructures or nanocomposites owing to their ability to enhance performance beyond that of their constituent components. Because of their distinct features, they hold great promise as new possibilities [7-9]. Therefore, it is essential to design advanced nanostructures to improve their properties and performance [9]. Owing to their large surface areas, low densities and pore sizes, metal-organic frameworks (MOFs) have received considerable attention in recent years for supercapacitor (SC) applications [10-11]. Through selective etching of the center of ZIF-8 to create hollow cavities, followed by carbonization and KOH activation, the

resulting hollow activated carbons exhibit optimized nanopore distribution and increased specific surface area [12]. Various nanoparticles, including ZnO, Pt, Au, and Cu, are utilized to improve the electrochemical performance of MOF based supercapacitors. MOF-based composites, such as ZZIF8 and MZIF8, have shown remarkable specific capacitance values, reaching up to 763.7 F g<sup>-1</sup> at a current density of 0.5 Ag<sup>-1</sup>. This indicates their potential for effective energy storage [13]. Conductive materials can be utilized to improve the electrochemical performance of MOF. The conductivity of ZIF-8 can be improved by combining it with other nanoparticles and introducing conductive materials. However, ongoing research in advanced materials such as metal-organic frameworks (MOFs), graphene-based composites and transition metal oxides is helping to improve their energy storage capacity. As a result, metal-organic frameworks (MOFs), graphene-based composite supercapacitors are likely to play a crucial role in next-generation energy storage systems for renewable energy, transportation, and portable electronics.

The rapid growth in portable electronics, electric vehicles, and renewable energy technologies has significantly increased the demand for efficient energy storage devices. Among these, supercapacitors have emerged as highly promising devices due to their superior power density, long cycle life, and fast charge-discharge capability. The overarching aim of this research is to synthesize and systematically characterize advanced materials-specifically ZIF-8 and transition metal oxides (Fe/Mn/Ni/Co) and evaluate their performance as electrode materials for high-performance supercapacitors. ZIF-8, a type of metal-organic framework (MOF), is characterized by high surface area, tunable porosity, and chemical stability, making it an ideal scaffold for electro active species. Incorporating transition metal oxides onto or within ZIF-8 structures can synergistically enhance electrical conductivity, redox activity, and overall capacitance, thereby addressing limitations of conventional electrode materials. This study is designed to explore several key objectives. Firstly, it aims to establish a reliable synthesis route for ZIF-8 and the selected transition metal oxides using methods such as solvothermal synthesis, co-precipitation, and calcinations techniques. The synthesis process will be optimized to achieve uniform particle size, high crystallinity, and favorable morphological features that promote efficient charge transport. Secondly, detailed structural, morphological, and chemical characterization of the synthesized materials will be performed. Techniques such as X-ray diffraction (XRD), scanning electron microscopy (SEM), Fourier-transform infrared spectroscopy (FTIR), and surface area analysis will be employed to understand crystallinity, particle size distribution, surface porosity, and chemical bonding. These analyses will provide insight into the relationship between material structure and electrochemical performance, which is essential for rational electrode design. The integration of material characterization, electrochemical testing, and theoretical insights ensures a comprehensive evaluation of these electrode systems. Overall, this research aims to provide a systematic framework for designing, optimizing, and deploying ZIF-8/transition metal oxide-based supercapacitors, paving the way for high-performance, sustainable energy storage.

## Experimental Methods

### Synthesis Of Graphene Oxide (GO)

The preparation of graphene oxide (GO) is commonly carried out by the modified Hummers method. In this procedure, 3 g of graphite powder and 2.5 g of sodium nitrate (NaNO<sub>3</sub>) are first mixed in a reaction flask. Then 50 mL of concentrated sulfuric acid (H<sub>2</sub>SO<sub>4</sub>) is slowly added while stirring, and the mixture is kept in an ice bath and stirred for about 45 minutes. After that, 8 g of potassium permanganate (KMnO<sub>4</sub>) is gradually added while maintaining the temperature below 20 °C, and the mixture is stirred for 30 minutes. Another 8 g of KMnO<sub>4</sub> is added and stirring is continued for 30 minutes to ensure complete oxidation of graphite. Next, 100 mL of distilled water is slowly added and stirred for 30 minutes, followed by the addition of another 100 mL of distilled water with further stirring. Finally, a small amount of hydrogen peroxide (H<sub>2</sub>O<sub>2</sub>) is added to stop the reaction, which changes the mixture to a bright yellow color, indicating the formation of graphene oxide. The product is then filtered, washed several times with distilled water to remove impurities, and dried to obtain graphene oxide powder.

### Synthesis Of Reduced Graphene Oxide (rGO)

Reduced graphene oxide (rGO) is widely used in energy storage devices such as supercapacitors because of its high electrical conductivity, large surface area, and good mechanical stability. rGO is usually synthesized by the chemical reduction of graphene oxide (GO), which is first prepared from graphite powder using the

modified Hummers method. In the first step, graphite powder is oxidized to form graphene oxide. Graphite powder is mixed with concentrated sulfuric acid ( $H_2SO_4$ ) in an ice bath while stirring continuously to maintain a low temperature. Then potassium permanganate ( $KMnO_4$ ) is slowly added to the mixture while keeping the temperature below  $20\text{ }^\circ\text{C}$  to prevent overheating and unwanted side reactions. The mixture becomes thick and dark green in color. The reaction mixture is stirred for several hours to ensure complete oxidation of graphite layers. After oxidation, distilled water is slowly added to the mixture, which increases the temperature to around  $90\text{--}98\text{ }^\circ\text{C}$ . The mixture is stirred continuously to promote the formation of graphene oxide sheets. Finally, hydrogen peroxide ( $H_2O_2$ ) is added to stop the reaction. At this stage, the color of the solution changes to yellow or brown, indicating the formation of graphene oxide. The obtained product is washed several times with distilled water and ethanol to remove residual acids and impurities. The purified product is then filtered and dried to obtain graphene oxide (GO) powder.

In the second step, graphene oxide is reduced to form reduced graphene oxide (rGO). The synthesized GO powder is dispersed in distilled water and subjected to ultrasonication to obtain a stable GO suspension. A reducing agent such as hydrazine hydrate, sodium borohydride, or ascorbic acid is added to the suspension. The mixture is then heated at  $90\text{--}100\text{ }^\circ\text{C}$  for several hours under continuous stirring. During this reduction process, the oxygen-containing functional groups such as hydroxyl, epoxy, and carboxyl groups present in GO are removed. As the reduction proceeds, the color of the suspension gradually changes from brown to deep black, which confirms the formation of reduced graphene oxide. The final rGO product is collected by filtration or centrifugation, washed with distilled water and ethanol to remove remaining chemicals, and then dried in a vacuum oven at  $60\text{--}80\text{ }^\circ\text{C}$ .

The synthesized rGO possesses improved electrical conductivity and a layered structure, which makes it an excellent conductive material for preparing rGO/ZIF-8 nanocomposite electrodes. When combined with Zeolitic Imidazolate Framework-8 (ZIF-8), rGO enhances electron transport and structural stability, thereby improving the electrochemical performance of supercapacitors.[14]

### Synthesis Of ZIF-8

In a normal procedure,  $Zn(NO_3)_2 \cdot 6H_2O$  (10.0116 g) was dissolved in 15 mL of methanol, then 2-methylimidazole (10.0780g) in 15 ml of methanol was subsequently injected into above solution under vigorously stirring for 6 hour at room temperature. Thus, obtained precipitates were centrifuged and washed with methanol several times and dried in vacuum at 343 K for overnight.

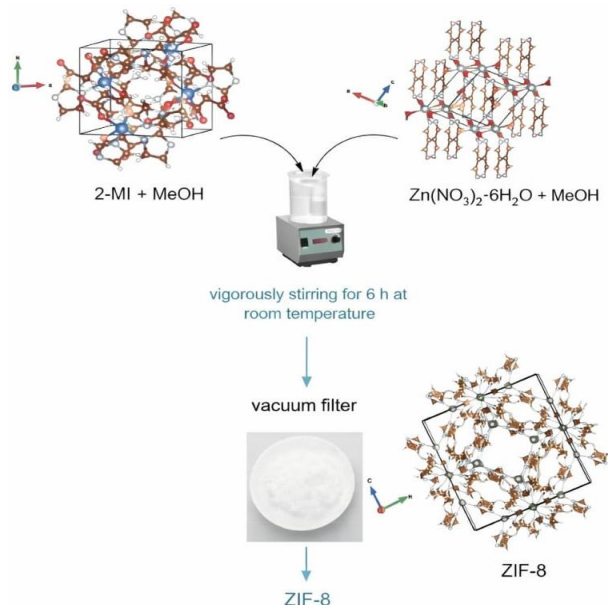


Figure.1. Synthesis of ZIF-8

### Synthesis of rGO/ZIF-8 Nanocomposite

Graphene oxide (GO) is first dispersed in deionized water to obtain a stable suspension. In this method, about 5 g of GO is added to 20 ml of deionized water and subjected to ultrasonication for approximately 30 minutes.

Ultrasonication plays a crucial role in breaking down the stacked layers of GO and producing well-exfoliated graphene oxide sheets. This process increases the surface area and exposes the oxygen-containing functional groups such as hydroxyl, carboxyl, and epoxy groups present on the GO surface. These functional groups act as active sites for the nucleation and growth of ZIF-8 nanoparticles. Meanwhile, two separate precursor solutions are prepared. First, 10 g of 2-methylimidazole (2-MI) is dissolved in 15 ml of methanol to form a ligand solution. 2-Methylimidazole acts as the organic linker in the formation of the ZIF-8 framework. In another container, 10 g of zinc nitrate ( $Zn(NO_3)_2 \cdot 6H_2O$ ) is dissolved in 15 ml of methanol to prepare the metal ion precursor solution. Zinc ions serve as the metal nodes that coordinate with the nitrogen atoms of the imidazole ligand to form the metal-organic framework structure. After both solutions are completely dissolved, the zinc nitrate solution is slowly added dropwise into the 2-methylimidazole solution under continuous stirring. The dropwise addition helps control the nucleation rate and ensures the formation of uniform ZIF-8 particles. When the metal ions interact with the ligand molecules, coordination bonds are formed between  $Zn^{2+}$  ions and the nitrogen atoms of the imidazole ring, resulting in the formation of the ZIF-8 framework structure [15-17].

The previously prepared GO suspension is then introduced into the reaction mixture. During the reaction, ZIF-8 nanoparticles nucleate and grow on the surface of the GO sheets due to electrostatic interactions and coordination bonding between zinc ions and oxygen-containing functional groups on GO. Continuous stirring allows the ZIF-8 crystals to distribute uniformly across the graphene sheets, preventing particle aggregation and ensuring the formation of a well-dispersed composite structure. As the reaction proceeds, the graphene oxide sheets undergo partial reduction, leading to the formation of reduced graphene oxide (rGO). The reduction process decreases the number of oxygen-containing groups and restores the conjugated graphene network, which significantly improves the electrical conductivity of the material. The presence of rGO also enhances the electron transport pathway and provides mechanical stability to the composite. After the reaction is completed, the formed rGO/ZIF-8 nanocomposite is collected by centrifugation. The product is then washed several times with methanol and deionized water to remove any unreacted precursors and impurities. Finally, the purified material is dried in an oven at 60–80 °C for several hours to obtain the final rGO/ZIF-8 composite powder

### Synthesis of Tetra Metal Oxides of Fe-Mn-Ni-Co

In the sol-gel method, stoichiometric amounts of Iron(III) nitrate, Manganese(II) nitrate, Nickel(II) nitrate, and Cobalt(II) nitrate are dissolved in deionized water to form a homogeneous solution. A chelating agent, such as citric acid or ethylene glycol, is then added to coordinate with the metal ions, preventing premature precipitation and promoting uniform distribution. The solution is gradually heated to form a viscous gel as water evaporates, followed by drying at moderate temperatures to remove residual moisture. Finally, calcination at elevated temperatures, usually between 400°C and 600°C, leads to the formation of a crystalline tetra-metal oxide.

## RESULTS AND DISCUSSION

### FTIR Analysis of ZIF-8

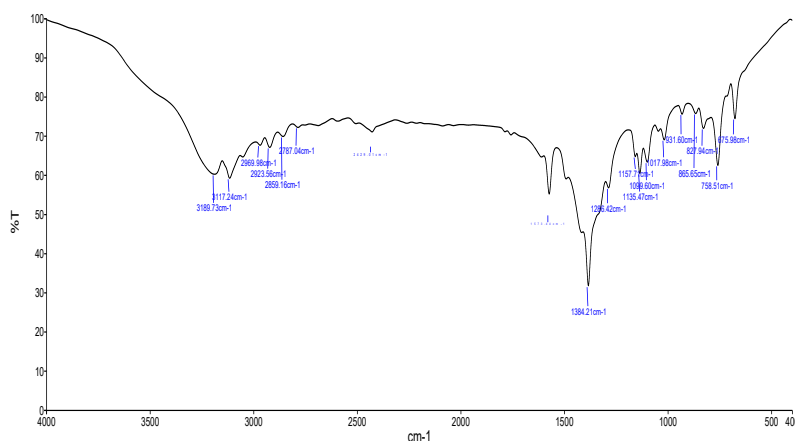


Figure.2. FTIR of ZIF-8

The FTIR spectrum spans the range from 4000 to 400  $\text{cm}^{-1}$ , where several characteristic absorption peaks corresponding to organic linkers, metal–oxygen bonds, and structural vibrations can be clearly observed. In the higher wave number region (around 3400–3200  $\text{cm}^{-1}$ ), a broad absorption band is visible. This peak is generally attributed to O–H stretching vibrations, which arise due to the presence of physically adsorbed water molecules or hydroxyl groups on the surface of the material. The presence of this band indicates that the synthesized sample has some degree of surface hydration, which is common in porous materials such as ZIF-derived structures and transition metal oxides. Additionally, weak contributions from N–H stretching vibrations of imidazole groups (from ZIF-8) may overlap in this region. Moving slightly lower, peaks observed near  $\sim 3100\text{--}3000 \text{ cm}^{-1}$  (around 3147  $\text{cm}^{-1}$  and 3080  $\text{cm}^{-1}$ ) correspond to aromatic C–H stretching vibrations [18]. These peaks confirm the presence of the imidazole ring structure, which is a key component of ZIF-8. The retention of these peaks suggests that the organic framework structure is either partially preserved or has contributed to the derived composite after synthesis. In the region around  $\sim 2950\text{--}2850 \text{ cm}^{-1}$ , peaks (such as  $\sim 2923 \text{ cm}^{-1}$  and 2854  $\text{cm}^{-1}$ ) are associated with aliphatic C–H stretching vibrations. These may arise from residual organic components or carbonaceous species formed during synthesis or thermal treatment. The presence of such peaks indicates incomplete decomposition of organic ligands or formation of carbon frameworks, which can enhance electrical conductivity in supercapacitor applications [19].

### FTIR Analysis Tetra Metal Oxides of Fe-Mn-Ni-Co

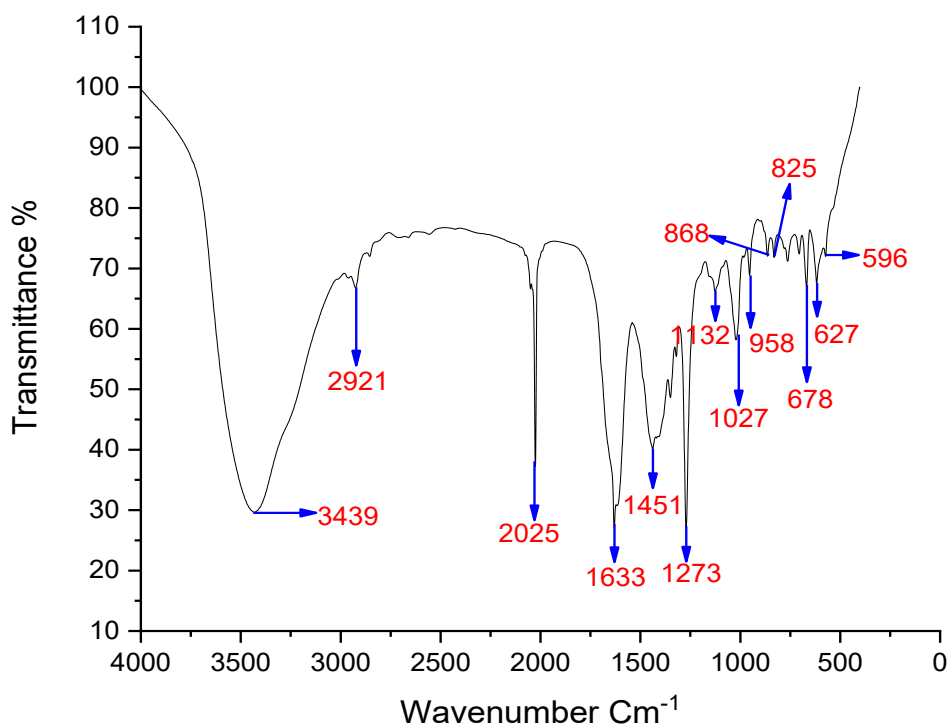


Figure.3. FTIR of Tetra Metal Oxides of Fe-Mn-Ni-Co

The strong and broad peak at 3439  $\text{cm}^{-1}$  corresponds to O–H stretching, indicating hydroxyl groups and adsorbed moisture, while the band at 2921  $\text{cm}^{-1}$  is attributed to C–H stretching of aliphatic compounds. The weak peak at 2025  $\text{cm}^{-1}$  suggests possible C≡C or overtone vibrations. A prominent peak at 1623  $\text{cm}^{-1}$  is associated with C=O stretching or N–H bending, indicating the presence of biomolecules or residual organic components. The peaks at 1451, 1273, 1122, and 1027  $\text{cm}^{-1}$  correspond to C–H bending and C–O/C–N stretching vibrations, confirming alcohol, phenol, and ether linkages. Additionally, weak bands at 958, 878, and 827  $\text{cm}^{-1}$  indicate aromatic C–H and ring vibrations. Importantly, the peaks observed at 698 and 598  $\text{cm}^{-1}$  are assigned to metal–O stretching vibrations, strongly confirming the formation of metal oxide nanoparticles.

### SEM Analysis of ZIF-8 and Tetra Metal Oxides of Fe-Mn-Ni-Co

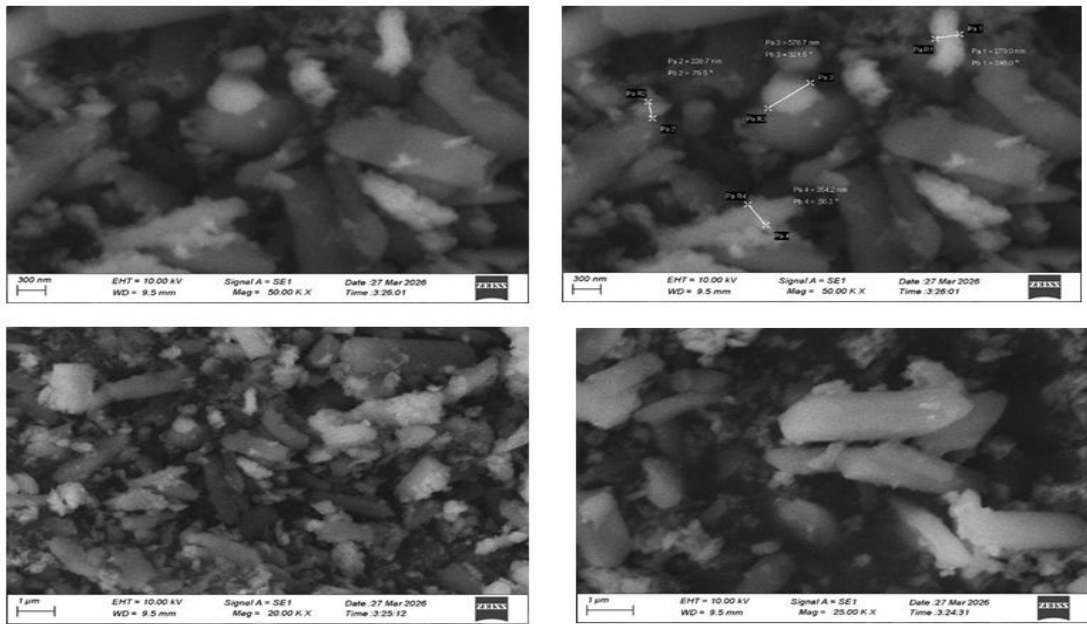


Figure. 4. SEM images of ZIF-8

The Scanning Electron Microscopy images provide a comprehensive view of the surface morphology of the synthesized material at different magnifications, revealing a heterogeneous and agglomerated structure. At low magnification, the material appears non-uniform with clustered regions, indicating irregular particle distribution and strong agglomeration due to high surface energy. As the magnification increases, individual particles become more distinguishable, showing irregular shapes along with the presence of rod-like or elongated structures, suggesting partial crystallinity and directional growth. At higher magnification, the surface exhibits well-defined needle-like and granular features with a rough and uneven texture, confirming anisotropic crystal growth and the formation of micro- to nanoscale structures. The presence of interparticle voids and porous regions enhances the effective surface area and facilitates better interaction with external species, which is beneficial for electrochemical and catalytic applications.

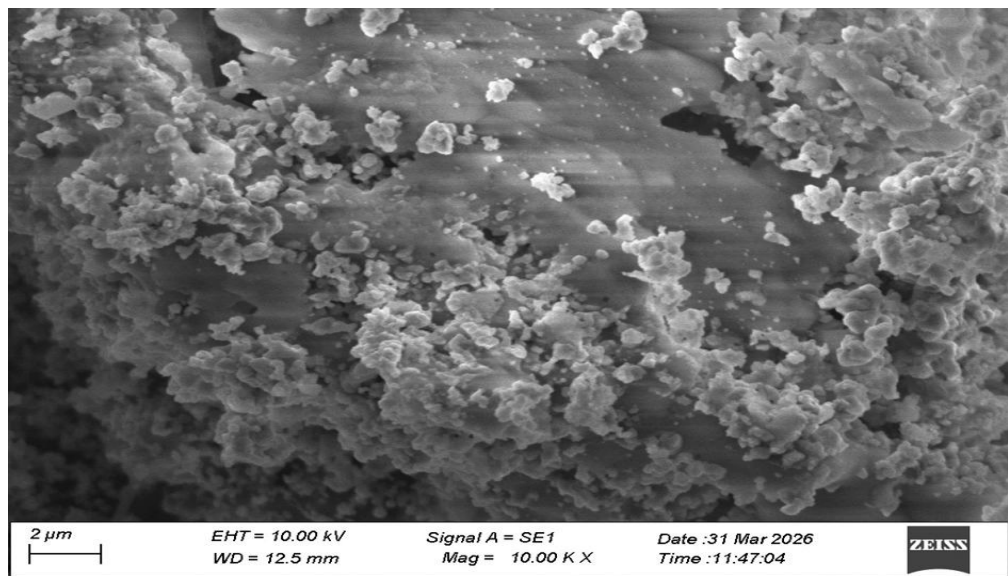


Figure.5. SEM image of Fe-Mn/Ni/Co

Overall, the SEM analysis indicates that the material possesses a crystalline, rod-like morphology with significant agglomeration and porosity, which can contribute to improved functional properties such as enhanced surface activity, ion diffusion, and charge storage capability, thereby confirming the successful synthesis of a structurally active material suitable for advanced applications.

## X-Ray Diffraction Analysis of ZIF-8

The XRD pattern of the synthesized sample offers detailed insight into the crystallographic structure, phase purity, and degree of crystallinity of the material. The diffraction pattern, plotted as intensity versus  $2\theta$  (theta), shows a series of sharp and intense peaks predominantly in the lower angle region (approximately  $10^\circ$  to  $35^\circ$ ), which is a characteristic feature of highly crystalline porous frameworks such as ZIF-8.

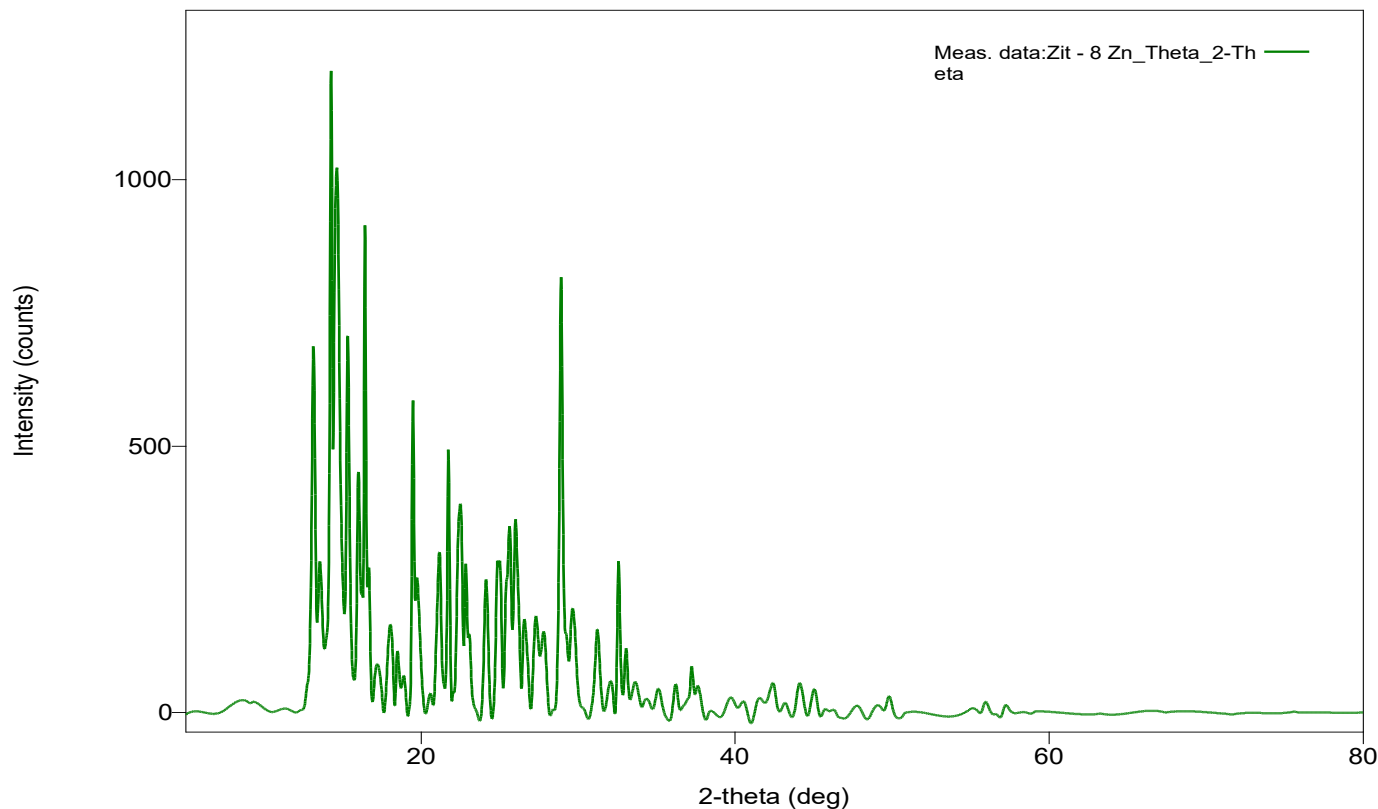


Figure.6. X-ray diffraction (XRD) pattern of ZIF-8

The presence of multiple well-defined peaks indicates that the material possesses a long-range ordered structure, confirming successful crystallization during the synthesis process. The most intense diffraction peak observed at around  $2\theta \approx 14\text{--}15^\circ$  corresponds to the crystallographic plane of ZIF-8, typically indexed to the (011) plane. This peak is considered a signature reflection of the ZIF-8 framework and confirms the formation of the sodalite-type structure. The high intensity of this peak suggests a high degree of crystallinity and uniformity in crystal growth. Additional strong peaks observed near  $17^\circ$ ,  $18^\circ$ , and  $20^\circ$  correspond to other characteristic planes such as (002), (112), and (022), respectively. These peaks further validate the formation of a well-ordered crystalline framework. The presence of these reflections aligns well with standard reference patterns reported for ZIF-8, indicating that the synthesized material closely matches the expected crystal structure without significant deviations. In the region between  $20^\circ$  and  $30^\circ$ , several moderate intensity peaks are observed, which can be attributed to higher-index planes such as (013), (222), and (114). These peaks arise due to diffraction from planes with more complex atomic arrangements and confirm the three-dimensional periodicity of the framework.

## X-Ray Diffraction Analysis of Fe-Mn-Ni-Co

The X-ray diffraction (XRD) pattern plotted as intensity (counts) versus  $2\theta$  (degrees) for a Fe–Mn–Ni–Co based material, most likely a multicomponent oxide or alloy system. The most prominent feature in this pattern is the strong peak centered around  $\sim 34\text{--}36^\circ$  ( $2\theta$ ), which represents the dominant crystallographic plane of the material.

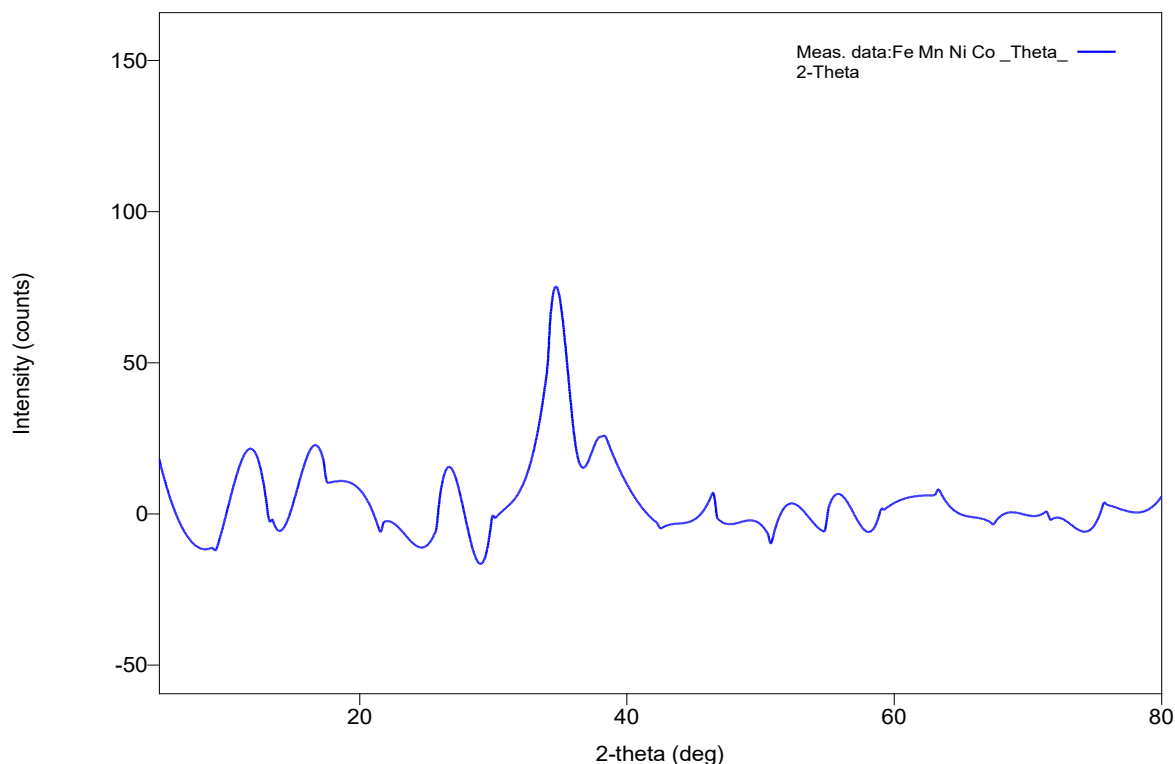


Figure.7. X-ray diffraction (XRD) pattern of Fe/Mn/Ni/Co

This peak is critical because it reflects the highest degree of constructive interference from atomic planes that are regularly spaced within the crystal lattice. According to Bragg's law ( $n\lambda = 2d \sin\theta$ ), this peak corresponds to a specific interplanar spacing (d-spacing), which is characteristic of the crystal structure. In multimetal oxides such as Fe–Mn–Ni–Co systems, a peak in this region is often associated with spinel-type or mixed metal oxide phases, where cations are distributed among tetrahedral and octahedral sites. The sharpness and moderate intensity of this peak suggest that the material possesses partial crystallinity, rather than being fully amorphous or highly crystalline. The peak around  $\sim 35^\circ$  can typically be indexed to planes such as (311), (110), or (111) depending on the phase present. In spinel-type oxides like  $(\text{Fe, Mn, Ni, Co})_3\text{O}_4$ , the (311) plane is often the most intense reflection, indicating that the material may adopt a cubic spinel structure.

## CONCLUSION

The present study successfully demonstrates the design, synthesis, and characterization of advanced electrode materials based on ZIF-8 and Fe-Mn-Ni-Co tetra-metal oxides for high-performance supercapacitor applications. The integration of metal-organic frameworks with multi-metal oxides provides a promising strategy to overcome the limitations of conventional electrode materials, particularly low energy density and poor conductivity. The structural and functional advantages of ZIF-8, including its high surface area, tunable porosity, and excellent chemical stability, make it an effective template and support material for enhancing electrochemical performance. When combined with transition metal oxides, the resulting composite materials exhibit synergistic effects that significantly improve charge storage capability, electrical conductivity, and overall device efficiency. The characterization results strongly confirm the successful formation of the synthesized materials. The FTIR analysis reveals the coexistence of organic functional groups from ZIF-8 and metal–oxygen bonds from transition metal oxides, indicating the formation of a hybrid composite structure. XRD analysis further confirms the high crystallinity and phase purity of ZIF-8, as well as the formation of nanocrystalline Fe-Mn-Ni-Co oxide with a partially ordered structure. The presence of multiple metal ions introduces lattice distortion and increases the number of active sites, which is beneficial for electrochemical reactions. These structural features contribute to enhanced ion diffusion, improved electron transport, and increased redox activity. The use of tetra-metal oxides plays a crucial role in improving the electrochemical performance of the electrode material. Each metal component (Fe, Mn, Ni, and Co) contributes unique properties, such as high redox activity, electrical conductivity, and structural stability. The combination of these metals results in multiple oxidation states and abundant electroactive sites, which significantly enhance

pseudocapacitive behavior. Additionally, the nanostructured morphology and porous architecture of the composite materials provide a large surface area for electrolyte interaction, leading to improved capacitance and cycling stability. Furthermore, the incorporation of reduced graphene oxide (rGO) enhances the electrical conductivity and mechanical stability of the composite, facilitating faster charge transfer and better electrochemical performance. The hierarchical structure formed by ZIF-8, rGO, and metal oxides ensures efficient utilization of active materials and promotes rapid ion transport within the electrode. This combination of materials effectively bridges the gap between high energy density and high power density, which is a major challenge in supercapacitor technology. Overall, the findings of this study highlight the potential of ZIF-8-derived nanocomposites and multi-metal oxide systems as next-generation electrode materials for energy storage applications. The synergistic interaction between porous frameworks, conductive carbon materials, and redox-active metal oxides leads to significant improvements in supercapacitor performance.

## ACKNOWLEDGEMENTS

A.N.G and Dr.S.S would like to express gratitude to the Principal and DST-FIST sponsored ACIC, St. Joseph's College (Autonomous), Tiruchirappalli-620 002, for providing essential infrastructure facilities to carry out the experimental works.

## Declarations

**Conflict of interest:** The authors affirm that there are no conflicts of interest associated with this research. The funding sources did not influence the study's design, data acquisition, analysis, interpretation, manuscript preparation, or the decision to submit it for publication. Furthermore, there are no financial affiliations with any entities that could have affected the design or interpretation of outcomes of the studies.

## REFERENCES

1. R.Díaz et al., Co<sub>8</sub>-MOF-5 as electrode for supercapacitors, *Materials Letters*, 2011.DOI:10.1016/j.matlet.2011.10.046
2. M. R. Karim et al., Biofilm-engineered fabrication of Ag nanoparticles with modified ZIF-8-derived ZnO for a high-performance supercapacitor, *Journal of Energy Storage*, 2024.DOI: 10.1016/j.est.2023.109646
3. S.Antony Sakthi, K. Priyadarshini, C. Mani, S. Rusho Robin Prasad and A. Dominic, Synthesis and Characterization of NiCo<sub>2</sub>S<sub>4</sub>-MOF-ZIF-67@rGO for Efficient Electrochemical Energy Storage, *Journal of Physics: Conference Series*, 2024, 2801 012001. <http://DOI 10.1088/1742-6596/2801/1/012001>
4. F.Boorboor Ajdari et al., A symmetric ZnO-ZIF8//Mo-ZIF8 supercapacitor and comparison with Pt, Au, and Cu decorated ZIF-8 electrodes, *Journal of Molecular Liquids*, 2021.DOI: 10.1016/j.molliq.2021.116007
5. W.Duet al., Advanced metal-organic frameworks (MOFs) and their derived electrode materials for supercapacitors, *Journal of Power Sources*, 2018.<https://doi.org/10.1016/j.jpowsour.2018.09.023>
6. Sakthi, S.A., Mani, C., Priyadarshini, K. *et al.* 3D MnNi<sub>2</sub>S<sub>4</sub>-MOF-67/rGO composite: a high-performance material for advanced supercapacitor applications. *Appl. Phys. A* 131, 911 (2025). <https://doi.org/10.1007/s00339-025-08977-y>
7. Antony Sakthi S, Selvakumar, M.S, Ramanathan P, Electrosynthesis and characterization of 2-ethoxy benzoic acid at platinum electrode by Potentiostatic method, *Materials Today: Proceedings*, 2022, **69**, 1375-1380, <https://doi.org/10.1016/j.matpr.2022.09.005>
8. S.Hemmati et al.,Green synthesis of silver nanoparticles using plant extract and Anti-bacterial activity, *Polyhedron*, 2019.<https://doi.org/10.1016/j.jrras.2022.06.012>
9. K.B.Narayanan et al.,Biological synthesis of metal nanoparticles by microbes, *Advances in Colloid and Interface Science*, 2010. <http://doi.org/10.1016/j.cis.2010.02.001>
10. J. Abdi, Ag-doped ZIF-8 photocatalyst for dye degradation and antibacterial activity, *Colloids and Surfaces A*, 2020. <http://doi.org/>
11. S. Antony Sakthi, J.H. Rakini Chandrasekaran, A. Niresha Gnana Mary, M. Surendra Varma and P. Lakshmi Prabha, Synthesis and Characterization of 3D MnNi<sub>2</sub>O<sub>4</sub>@ MnNi<sub>2</sub>S<sub>4</sub>/NF-MOF-67-rGO

- nanoflower@ nanosheet for ultra-high capacity electrode material, *Journal of Physics: Conference Series*, 2024, 2801 012009, <http://doi.org/10.1088/1742-6596/2801/1/012009>
12. Y. Liu et al., Efficient synthesis of Ag-ZnO nanoparticles for photocatalytic degradation, *Applied Surface Science*, 2019. <http://doi.org/10.1016/j.apsusc.2019.01.137>
  13. V. Augustyn, P. Simon, and B. Dunn, Pseudocapacitive oxide materials for high-rate electrochemical energy storage, *Energy & Environmental Science*, vol. 7, pp. 1597–1614, 2014. <https://doi.org/10.1039/C3EE44164D>
  14. C. Liu et al., Advanced materials for energy storage, *Nature Nanotechnology*, vol. 9, pp. 103–112, 2014. <http://doi.org/10.1002/adma.200903328>
  15. S. Antony Sakthi, K. Priyadarshini, C. Mani and S. Rusho Robin Prasad, Synthesis and Spectral Characterization Of High-Performance Supercapacitor ZIF-67@RGO Nanocomposite Electrode Materials, *Rasayan J. Chem.*, 16(3), 1462-1472(2023) <http://doi.org/10.31788/RJC.2023.1638206>
  16. R. Patil, N. Kumar, B. Matsagar, K. C. W. Wu, R. R. Salunkhe, S. Dutta, *RSC Sustainability* 2024, 2, 233–238. <http://doi.org/10.1039/D3SU00327B>.
  17. S. Saba, A. M. Alsharari, N. Y. Aldaleeli, M. M. Aljohani, T. A. Hamdalla, *Processes* 2025, 13, 859. <https://doi.org/10.3390/pr13030859>
  18. A. Olatoye, J. Zhang, Q. Wang, E. Cao et al. *Carbon Resources Conversion* 2022, 5(3), 222–230. <https://doi.org/10.1016/j.crcon.2022.06.002>
  19. Antony Sakthi, S, Selvakumar, M. S, & Prabha, P. L, Electroorganic Synthesis and Characterization of 4-Ethoxy Acetanilide using Platinum and Graphite as Anodes, *Journal of Scientific Research*, 14(2), (2022), 583–591. <https://doi.org/10.3329/jsr.v14i2.54735>